Int. J. Solids Structures Vol. 25, No. 6, pp. 591–607, 1989
Printed in Great Britain.

0020-7683/89 $3.00 + .00

THREE-DIMENSIONAL ELASTIC CRACK TIP INTERACTIONS WITH SHEAR TRANSFORMATION STRAINS

B. L. KARIHALOO and XIAOFAN HUANG
School of Civil and Mining Engineering, The University of Sydney, N.S.W 2006, Australia

(*Received* 3 *May* 1988)

Abstract—Three-dimensional elastic interactions between a half-plane crack and sources of internal stress such as unconstrained shear transformation strains are analysed using Bueckner's recent "weight function" method of three-dimensional crack analysis. Analytical expressions are given for the stress intensity factors induced along the crack front by unconstrained shear transformation strains for several simple shapes of the transformation domain centred at the origin. When the centre of the transformation domain is not coincident with the origin of coordinates analytical expressions are too cumbersome to be of much practical value. In such instances, numerical results are presented for transformation domains in the shape of a sphere and an oblate spheroid. The influence of the orientation of the latter is also studied.

1. INTRODUCTION

In the last few years considerable advances have been made in understanding the mechanism of transformation toughening of ceramics triggered by an elevated stress field such as that at a sharp crack front. In the majority of these studies (McMeeking and Evans, 1982; Budiansky *et al.*, 1983; Budiansky, 1983; Lambropoulos, 1986), the problem was modelled as a two-dimensional crack system subjected only to dilatational phase transformations in which the effect of transformed particles was "smeared" out over the whole transformed region. This continuum, two-dimensional plane stress approximation to what is essentially a discrete, three-dimensional problem is adequate if the number of transformed particles is large but unlikely to be valid if the transformed zone spans only a few particles.

Recently, Rice (1985) gave exact analytical expressions for the stress intensity factors in mode I due to three-dimensional elastic interactions between a half-plane crack and a source of internal stress such as transformation strains. Rice's treatment was generalized to modes I, II and III by Gao (1988) using the three-dimensional "weight functions" recently published by Bueckner (1987). It should be noted that the pioneering work reported by Rice (1985), and Gao (1988) is restricted to dilatational transformation strains for which the shape of transforming particles is irrelevant. It is however well-known (Lambropoulos, 1986) that shear strains, shape and orientation of the transforming particles also have a significant effect upon transformation toughening.

In the present paper which complements the work reported by Rice (1985), and Gao (1988) analytical expressions are given for stress intensity factors induced along a half-plane crack front by unconstrained shear components of transformation strains for several, simple shapes of the transforming particles. The analysis is based on Bueckner's three-dimensional "weight functions" (Buecker, 1987). Analytical treatment is practicable only when the transformation domain is centred at the origin. In all other cases the analytical expressions are too cumbersome to be of much practical value. In such instances, numerical results are presented for transformation domains in the shape of a sphere and an oblate spheroid. The influence of the orientation of the latter is also studied.

2. MATHEMATICAL PRELIMINARIES

Consider a half-plane crack in an infinite elastic solid. The crack lies on the plane $y = 0$ with its tip along z-axis such that the region $x < 0$ is cracked. Rice (1985) showed that the stress intensity factors $K_\alpha(z')$ at location z' along the crack front (α = I, II, III refer to

tensile, in-plane shear and anti-plane shear modes) due to a distribution of transformation strains ε^T_{mn} over a volume V may be written as

$$K_\alpha(z') = 2\mu \int_V U^\alpha_{mn}(x, y, z-z')\varepsilon^T_{mn}(x, y, z)\, dx\, dy\, dz \tag{1}$$

where μ is the shear modulus of the solid and U^α_{mn} is the fundamental stress field in mode α defined by

$$U^\alpha_{mn} = (h_{\alpha m,n} + h_{\alpha n,m})/2 + [\nu/(1-2\nu)]\delta_{mn} h_{\alpha j,j}. \tag{2}$$

In eqn (2) $\underline{h}_\alpha \equiv (\underline{h}_I, \underline{h}_{II}, \underline{h}_{III})$, with components $h_{\alpha i}$, are weight functions for a half-plane cracked body, δ_{mn} is the Kronecker delta, Latin indices range over x, y, z and when preceded by a comma denote differentiation with respect to that coordinate, and summation is implied by repeated indices. Expressions for U^α_{mn} may be found in the work by Gao (1988). An explicit solution for $\underline{h}_I$ was given by Rice (1985). Recently, Bueckner (1987) derived $\underline{h}_\alpha$ for all modes in terms of a Papkovitch–Neuber potential function $G(x, y, z)$.

$$G(x, y, z-z') = \frac{C_0}{\zeta} \ln\left(\frac{q+\zeta}{q-\zeta}\right) \tag{3}$$

where

$$\zeta = \sqrt{[x + i(z-z')]}, \quad q = \mathrm{Re}\sqrt{[2(x+iy)]} = \sqrt{(2\rho)}\cos\frac{\phi}{2}$$

and

$$\rho = \sqrt{(x^2+y^2)}, \quad \tan\phi = y/x \quad \text{and} \quad C_0 = -1/[4(1-\nu)\pi^{3/2}].$$

ρ and ϕ represent polar co-ordinates in the (x, z) plane such that the crack faces C^+ and C^- can be distinguished by $\phi = \pi$, $-\pi$, respectively.

In terms of $G(x, y, z-z')$, the x, y, z components of h_α are

$$\begin{aligned} h_{Ix} &= -(1-2\nu)G_{,x} - yG_{,xy} \\ h_{Iy} &= 2(1-\nu)G_{,y} - yG_{,yy} \\ h_{Iz} &= -(1-2\nu)G_{,z} - yG_{,zy}; \end{aligned} \tag{4}$$

$$\begin{aligned} h_{\beta x} &= -2(1-\nu)g_\beta + y\psi_{\beta,x} \\ h_{\beta y} &= -(1-2\nu)\psi_\beta + y\psi_{\beta,y} \quad \beta = II, III \\ h_{\beta z} &= -2(1-\nu)h_\beta + y\psi_{\beta,z}; \end{aligned} \tag{5}$$

where

$$\begin{aligned} (2-\nu)g_{II} &= -G_{,y} + 2(1-\nu)H_{,x} + 2iH_{,z} \\ (2-\nu)h_{II} &= -i(G_{,y} + 2H_{,x}) + 2(1-\nu)H_{,z} \\ (2-\nu)\psi_{II} &= -G_{,x} - iG_{,z} - 2(1-\nu)H_{,z}; \end{aligned} \tag{6}$$

$$\begin{aligned} (2-\nu)g_{III} &= i(1-\nu)(G_{,y} + 2H_{,x}) - 2H_{,z} \\ (2-\nu)h_{III} &= -(1-\nu)G_{,y} + 2H_{,x} + 2i(1-\nu)H_{,z} \\ (2-\nu)\psi_{III} &= i(1-\nu)(G_{,x} + iG_{,z} - 2H_{,y}) \end{aligned} \tag{7}$$

and

$$H = yG_{,x} - xG_{,y}. \tag{8}$$

For pure dilatational transformation strains

$$\varepsilon^T_{mn}(x, y, z) = \theta^T(x, y, z)\frac{\delta_{mn}}{3}, \tag{9}$$

eqn (1) is considerably simplified:

$$K^D_\alpha(z') = \frac{2\mu}{3}\int_V U^\alpha_{jj}\theta^T(x, y, z)\,dx\,dy\,dz, \tag{10}$$

where superscript D denotes dilatation. The problem of computing $K^D_\alpha(z')$ analytically was completely solved by Gao (1988). In this case U^α_{jj} are related only to $G_{,yy}$ and $\psi_{\beta,y}$ which are readily calculated.

$$U^I_{jj} = 2(1+\nu)\cos(\phi/2)\left[1 - 8\frac{\rho^2}{R^2}\sin^2(\phi/2)\right]\Big/A_0$$

$$U^\beta_{jj} = -2(1+\nu)\psi_{\beta,y} \quad (\beta = II, III) \tag{11}$$

where

$$\psi_{II,y} = \sin(\phi/2)\left[\frac{2-3\nu}{2-\nu} + 8\frac{\rho^2}{R^2}\left\{\cos^2(\phi/2) - \frac{1-\nu}{2-\nu}\right\}\right]\Big/A_0$$

$$\psi_{III,y} = 4\rho(z-z')\sin(\phi/2)/(A_0R^2) \tag{12}$$

and

$$R^2 = x^2 + y^2 + (z-z')^2, \quad A_0 = 2(1-\nu)(2\pi)^{3/2}\rho^{1/2}R^2.$$

In the present paper we complete the solution for unconstrained shear transformation strains with $\varepsilon^T_{mn} = \varepsilon^T_{nm}$ $(n \neq m)$, for which eqn (1) reduces to

$$K^S_\alpha(z') = 4\mu\int_V U^\alpha_{mn}\varepsilon^T_{mn}\,dx\,dy\,dz \quad (m \neq n) \tag{13}$$

where we have used the superscript S to identify the pure shear contribution to the stress intensity factors. If K^0_α denotes the mode α stress intensity factor induced at the crack front by external loading, then under any arbitrary (internal) transformation strain field and external loading the stress intensity factors may be obtained by superposition

$$K_\alpha(z') = K^0_\alpha(z') + K^D_\alpha(z') + K^S_\alpha(z'). \tag{14}$$

The calculation of stress intensity factors due to unconstrained shear transformation strains presents several difficulties because the derivatives of $G(x, y, z-z')$ with respect to x and z such as $G_{,xz}$, $G_{,xxz}$ and therefore the functions U^α_{ij} $(i, j \neq y)$ involve real and/or imaginary parts of log-like complex functions. General expressions for $G_{,xz}$ and $G_{,xxz}$ are given in Appendix A.

Formally, the expressions (13) may be reduced to the following non-dimensional form.

$$K_{\mathrm{I}}^{S}(z')=\frac{2}{(1+\nu)}\int_{V}\left\{\varepsilon_{xy}^{T}\frac{C_0 p}{4\rho R^2}\left[(1-\cos\phi-2\cos^2\phi)+4\frac{\rho^2}{R^2}(1-\cos\phi-2\cos^2\phi)\right.\right.$$
$$\left.+32\frac{\rho^4}{R^4}\cos\phi(1-\cos^2\phi)\right]-\varepsilon_{yz}^{T}\frac{C_0 p(z-z')}{R^4}\left[(1+\cos\phi)-8\frac{\rho^2}{R^2}(1-\cos^2\phi)\right]$$
$$\left.+\varepsilon_{zx}^{T}\frac{C_0 q(z-z')}{R^4}\left[(1-\cos\phi)+8\frac{\rho^2}{R^2}(\cos\phi-\cos^2\phi)\right]-\varepsilon_{zx}^{T}(1-2\nu)G_{,xz}\right\}\mathrm{d}V \tag{15}$$

$$K_{\mathrm{II}}^{S}(z')=\frac{2}{(1+\nu)}\int_{V}\left\{\varepsilon_{xy}^{T}\frac{C_0 q}{4\rho R^2(2-\nu)}\left[(2-3\nu)(-1+\cos\phi-2\cos^2\phi)\right.\right.$$
$$+4\frac{\rho^2}{R^2}(-\nu+(4-7\nu)\cos\phi-2(2-3\nu)\cos^2\phi)$$
$$\left.+32\frac{\rho^4}{R^4}(\nu\cos\phi+2(1-\nu)\cos^2\phi-(2-\nu)\cos^3\phi)\right]$$
$$-\varepsilon_{yz}^{T}\frac{C_0 q(z-z')}{4(2-\nu)\rho^2 R^2}\left[(-2+5\nu+(2-3\nu)\cos\phi)\frac{\rho^2}{R^2}\right.$$
$$\left.-8\frac{\rho^4}{R^4}(\nu+2(1-\nu)\cos\phi-(2-\nu)\cos^2\phi)\right]$$
$$+\varepsilon_{zx}^{T}\frac{C_0 p(z-z')}{4(2-\nu)\rho^2 R^2}\left[4\frac{\rho^2}{R^2}(4-13\nu+8\nu^2+\nu(3-4\nu)\cos\phi)\right.$$
$$\left.+32\frac{\rho^4}{R^4}(\nu\cos\phi+\nu(5-4\nu)\cos^2\phi+\nu\cos^3\phi)\right]$$
$$\left.-\varepsilon_{zx}^{T}\frac{2(1-\nu)(1-2\nu)}{(2-\nu)}yG_{,xxz}\right\}\mathrm{d}V \tag{16}$$

$$K_{\mathrm{III}}^{S}(z')=\frac{2}{(1+\nu)}\int_{V}\left\{\varepsilon_{xy}^{T}\frac{(1-\nu)C_0 q(z-z')}{(2-\nu)\rho^2 R^2}\left[(2-2\nu-2\cos\phi)\frac{\rho^2}{R^2}\right.\right.$$
$$\left.+16\frac{\rho^4}{R^4}(\cos\phi-\cos^2\phi)\right]-\varepsilon_{yz}^{T}\frac{(1-\nu)C_0 q}{2(2-\nu)\rho R^2}$$
$$\times\left[(2+\nu)+\frac{\rho^2}{R^2}(-32+(32-4\nu)\cos\phi)+32\frac{\rho^4}{R^4}(1-\cos\phi)\right]$$
$$-\varepsilon_{zx}^{T}\frac{(1-\nu)C_0 p}{2(2-\nu)\rho R^2}\left[-5\nu-(2-4\nu)\cos\phi-(4-8\nu)\cos^2\phi\right.$$
$$+\frac{\rho^2}{R^2}(-4+12\nu-(28+4\nu)\cos\phi-(16-32\nu)\cos^2\phi)$$
$$\left.+32\frac{\rho^4}{R^4}(\cos\phi+(1-2\nu)\cos^2\phi)\right]$$
$$\left.+\varepsilon_{zx}^{T}\frac{(1-\nu)(1-2\nu)}{(2-\nu)}y\ \mathrm{Im}\ (G_{,xxz})\right\}\mathrm{d}V \tag{17}$$

where

$$p = \text{Im}\ \sqrt{[2(x+iy)]} = \sqrt{(2\rho)}\ \sin\ (\phi/2). \tag{18}$$

To arrive at the non-dimensional form of stress intensity factors (15)–(17), we first introduced the non-dimensional variables identified by an asterisk

$$x^* = x/a, \quad y^* = y/a, \quad z^* = z/a, \quad K_{\mathrm{I}}^{*S}(z^{*\prime}) = K_{\mathrm{I}}^{S}(z')/(E\sqrt{a})$$

$$\mathrm{d}V^* = \mathrm{d}V/a^3, \quad G^*_{x^*z^*} = \frac{a^3}{\sqrt{a}} G_{,xz}, \quad G^*_{x^*x^*z^*} = \frac{a^4}{\sqrt{a}} G_{,xxz},$$

and then for brevity omitted the asterisk.

Calculation of K_{I}^S for any arbitrary V involves complicated integrands such as Re $(G_{,zzz})$, Im $(G_{,zzz})$ and Im $(G_{,zz})$ (Appendix A) which require numerical integration. However, the last term in the expression for $K_{\mathrm{I}}^S(z')$ will vanish if ε_{zx}^T is a function of y alone. Likewise, the last term in the expressions for $K_{\mathrm{II}}^S(z')$ and $K_{\mathrm{III}}^S(z')$ will vanish provided either ε_{zx}^T is a function of y alone or ε_{zx}^T is an even function of y and the region V is symmetric with respect to y (see Appendix B). The expressions are further simplified if the unconstrained shear transformation strains are functions of y alone and the region V is symmetric with respect to y. In this case, besides the last term involving $G(x, y, z)$, the terms containing the variable $p = \sqrt{2\rho}\ \sin\ (\phi/2)$ also vanish.

3. SIMPLE TRANSFORMATION DOMAINS

As mentioned above, for an arbitrary transformation domain V the integrals (15)–(17) must be evaluated numerically. In several instances however it is possible to express the integrals as infinite series, provided there is no contribution from the terms involving $G(x, y, z)$. In this section we will first demonstrate this "analytical" procedure on the spheroidal region (Fig. 1)

$$(x-x_0)^2 + y^2 + \frac{a^2}{c^2}(z-z_0)^2 \leqslant 1 \tag{19}$$

and then obtain complete solutions for the spheroidal region centred at the origin $(x_0 = y_0 = z_0 = 0)$. For the spheroidal region (19), and indeed for an arbitrary ellipsoidal region to be considered numerically in the next section, we introduce ellipsoidal coordinates $r, \theta, \bar{\phi}$

$$x = r\ \cos\ \theta\ \cos\ \bar{\phi}$$

$$y = \frac{b}{a}\, r\ \cos\ \theta\ \sin\ \bar{\phi}$$

$$z = \frac{c}{a}\, r\ \sin\ \theta \tag{20}$$

such that in general the coordinates of the centroid of region V, x_0, y_0, z_0 transform into r_0, θ_0, $\bar{\phi}_0$. We have used an overbar to distinguish the ellipsoidal coordinate $\bar{\phi}$ from the cylindrical coordinate ϕ appearing in integrals (15)–(17) and elsewhere. $\bar{\phi}$ is related to ϕ through

$$\cos\ \phi = \cos\ \bar{\phi} \Big/ \left(\cos^2\ \bar{\phi} + \frac{b^2}{a^2} \sin^2\ \bar{\phi}\right)^{1/2}. \tag{21}$$

For a spheroidal region, $\bar{\phi} = \phi$.

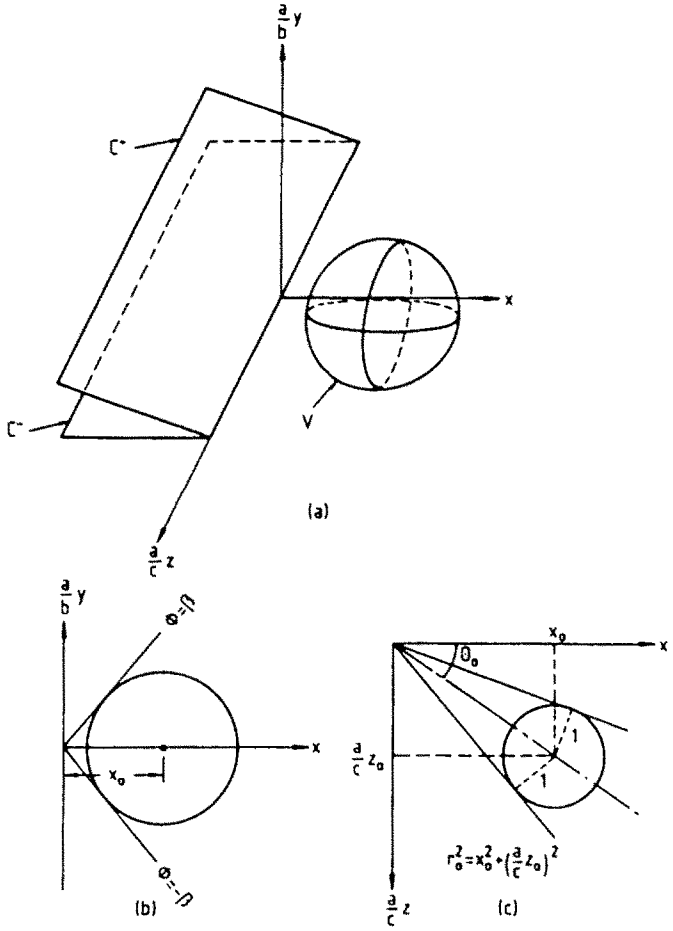

Fig. 1. A half-plane crack, and region V (with $a = b$, $y_0 = 0$) which has undergone transformation strains showing the Cartesian and ellipsoidal coordinate systems.

The lower (l) and upper (u) limits of integration for an arbitrary ellipsoidal region are calculated as follows.

For the radius $r = \left(x^2 + \frac{a^2}{b^2}y^2 + \frac{a^2}{c^2}z^2\right)^{1/2}$,

$$r_l \leqslant r \leqslant r_u \tag{22}$$

where

$$r_{u,l} = r_0 \cos\alpha \pm \sqrt{[(r_0 \cos\alpha)^2 - (r_0^2 - 1)]} \tag{23}$$

and α is the angle between radius vectors r_0 and r such that

$$\cos\alpha = \cos\theta \cos(\bar{\phi} - \bar{\phi}_0) + \sin\theta \sin\theta_0. \tag{24}$$

For $\rho_0 \geqslant 1$ (where $\rho_0 = [(x_0^2) + (ay_0/b)^2]^{1/2}$, not to be confused with cylindrical coordinate $\rho = (x^2 + y^2)^{1/2}$ appearing in integrals (15)–(17) and elsewhere),

$$F_0 - \beta = \bar{\phi}_l \leqslant \bar{\phi} \leqslant \bar{\phi}_u = F_0 + \beta \tag{25}$$

where

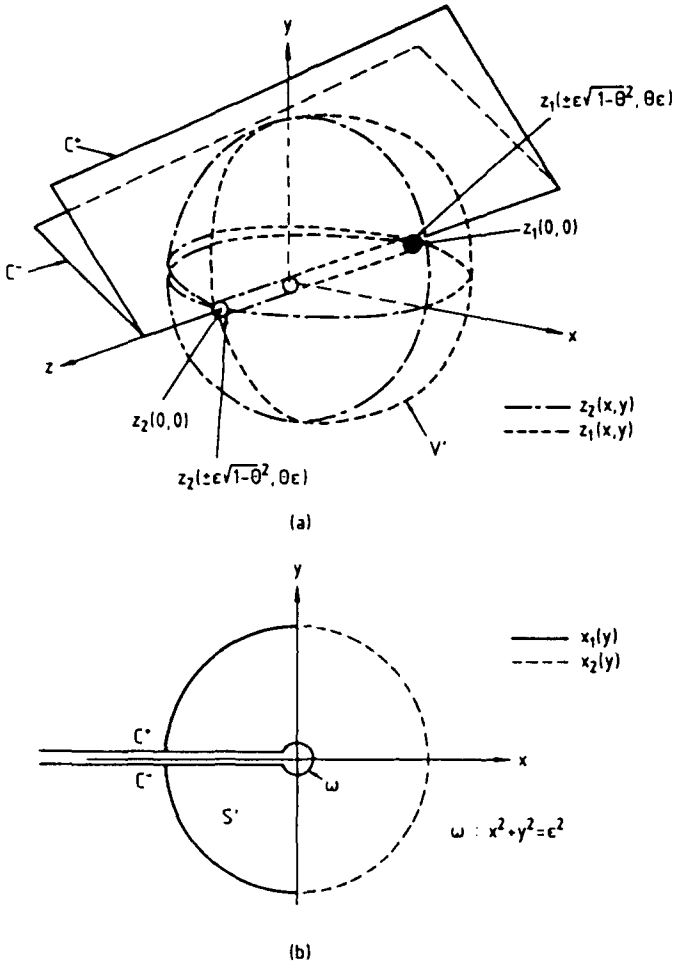

Fig. 2. The subregion V' consisting of the torus ω and certain portions of C^+, C^- and V.

$$\beta = \begin{cases} \sin^{-1}(1/\rho_0); & \rho_0 = 1 \\ 0; & y_0 = 0 \end{cases} \tag{26}$$

$$F_0 = \begin{cases} \tan^{-1}\left(\dfrac{ay_0}{bx_0}\right); & x_0 > 0 \\ \tan^{-1}\left(\dfrac{ay_0}{bx_0}\right) + \pi; & x_0 < 0. \end{cases} \tag{27}$$

For $\rho_0 < 1$, $-\pi \leqslant \bar{\phi} \leqslant \pi$. Finally, the limits on θ are calculated from the solution to the inequality

$$1 - r_0^2 \sin^2 \alpha \geqslant 0. \tag{28}$$

We note first that

$$\theta_0 = \begin{cases} 0; & z_0 = 0 \\ \pi/2; & \rho_0 = 0 \\ \tan^{-1}\left(\dfrac{z_0}{\rho_0 c}\right); & \text{otherwise.} \end{cases} \tag{29}$$

The lower and upper limits on θ following from the solution of (28) are given in Table 1.

In Table 1

$$\alpha_1^{\pm} = \tan^{-1}\left[\frac{-r_0^2\cos\theta_0\sin\theta_0\cos(\bar\phi-\bar\phi_0)\pm r_0\sqrt{[(r_0^2-1)\{1-r_0^2\cos^2\theta_0\sin^2(\bar\phi-\bar\phi_0)\}]}}{1-r_0^2\cos^2\theta_0}\right],$$

$$\alpha_2 = \tan^{-1}\left[\frac{r_0^2-1-\cos^2(\bar\phi-\bar\phi_0)}{r_0^2\sin 2\theta_0\cos(\bar\phi-\bar\phi_0)}\right]. \tag{30}$$

For the special region described by (19), $a = b$, $\bar\phi_0 = 0$ and $\bar\phi = \phi$, such that $\rho_0 = x_0$, $F_0 = 0$, thereby considerably simplifying the limits of integration. It should however be borne in mind that when $|x_0| \leqslant 0$ and $|x_0| < b$ the integrals have a meaning only in the mathematical sense. For $|x_0| \leqslant 0$ the integrals can be interpreted physically only when $|x_0| \geqslant b$. For the region (19) and constant transformation strains the integrals (15)–(17) simplify to read

$$K_{\mathrm I}^{S}(0) = \frac{8\sqrt{2}}{(1+\nu)}C_0\frac{c^2}{a^2}\varepsilon_{zx}^{T}\int_0^{\beta}\int_{\theta_l}^{\theta_u}F_{zx}^{\mathrm I}(\theta,\phi)\,\mathrm d\theta\,\mathrm d\phi \tag{31}$$

$$K_{\mathrm{II}}^{S}(0) = \frac{2\sqrt{2}}{(2-\nu)(1+\nu)}C_0\frac{c}{a}\varepsilon_{xy}^{T}\int_0^{\beta}\int_{\theta_l}^{\theta_u}F_{xy}^{\mathrm{II}}(\theta,\phi)\,\mathrm d\theta\,\mathrm d\phi$$
$$-\frac{8\sqrt{2}}{(2-\nu)(1+\nu)}C_0\frac{c^2}{a^2}\varepsilon_{yz}^{T}\int_0^{\beta}\int_{\theta_l}^{\theta_u}F_{yz}^{\mathrm{II}}(\theta,\phi)\,\mathrm d\theta\,\mathrm d\phi \tag{32}$$

$$K_{\mathrm{III}}^{S}(0) = \frac{8\sqrt{2(1-\nu)}}{(2-\nu)(1+\nu)}C_0\frac{c^2}{a^2}\varepsilon_{xy}^{T}\int_0^{\beta}\int_{\theta_l}^{\theta_u}F_{xy}^{\mathrm{III}}(\theta,\phi)\,\mathrm d\theta\,\mathrm d\phi$$
$$-\frac{4\sqrt{2(1-\nu)}}{(2-\nu)(1+\nu)}C_0\frac{c}{a}\varepsilon_{yz}^{T}\int_0^{\beta}\int_{\theta_l}^{\theta_u}F_{yz}^{\mathrm{III}}(\theta,\phi)\,\mathrm d\theta\,\mathrm d\phi \tag{33}$$

where ($m \neq n$, $a = \mathrm I, \mathrm{II}, \mathrm{III}$)

$$F_{mn}^{\alpha} = (\sqrt{r_u}-\sqrt{r_l})b_k a_{ki}^{(c)}[U_{mn}^{\alpha}](\cos\theta/\sin\theta)\frac{\cos(\phi/2)}{\sqrt{\cos\theta}}\cos^{l}\phi \tag{34}$$

and "/" between c/s and between $\cos\theta/\sin\theta$ means that either $\cos\theta$ or $\sin\theta$ term appears in (34) together with the corresponding coefficient $a_{ki}^{(c)}[U_{mn}^{\alpha}]$ or $a_{ki}^{(s)}[U_{mn}^{\alpha}]$.

Table 1. Lower and upper limits on θ

r_0			θ_l	θ_u
<1			$-\pi/2$	$\pi/2$
1	$\theta_0 = \alpha$		$-\pi/2$	$\pi/2$
	$\theta_0 = \pi/2$		0	$\pi/2$
	$\theta_0 = -\pi/2$		$-\pi/2$	0
	$\pi/2 > \theta_0 > 0$		$-\tan^{-1}[\cos(\bar\phi-\bar\phi_0)/\tan\theta_0]$	$\pi/2$
	$0 > \theta_0 > -\pi/2$		$-\pi/2$	$-\tan^{-1}[\cos(\bar\phi-\bar\phi_0)\tan\theta_0]$
>1	$\rho_0 < 1$	$z_0 \geqslant 0$	α_1^{+}	$\pi/2$
		$z_0 < 0$	$-\pi/2$	α_1
	$\rho_0 = 1$	$z_0 \geqslant 0$	α_2	$\pi/2$
		$z_0 < 0$	$-\pi/2$	α_2
	$\rho_0 > 1$		α_1^{+}	α_1

In (34), $k = 0, 1, 2$ and $i = 0, 1, 2, 3$ and

$$b_k = \frac{\cos^{2k}\theta}{\left(\cos^2\theta + \frac{c^2}{a^2}\sin^2\theta\right)^{k+1}}. \tag{35}$$

The only non-zero coefficients $a^c_{ki}[U^{\mathrm{I}}_{mn}]$ and $a^s_{ki}[U^{\mathrm{I}}_{mn}]$ are

$$a^s_{ki}[U^{\mathrm{I}}_{xz}]: \quad a^s_{10} = 1, \quad a^s_{11} = -1, \quad a^s_{21} = 8, \quad a^s_{22} = -8 \tag{36}$$

$$\begin{aligned} a^c_{ki}[U^{\mathrm{II}}_{xy}]: \quad & a^c_{00} = -(2-3\nu), \quad a^c_{01} = (2-3\nu), \quad a^c_{02} = -2(2-3\nu) \\ & a^c_{10} = -4\nu, \quad a^c_{11} = 4(4-7\nu), \quad a^c_{12} = -8(2-3\nu) \\ & a^c_{21} = 32\nu, \quad a^c_{22} = 64(1-\nu), \quad a^c_{23} = -32(2-\nu) \end{aligned} \tag{37}$$

$$a^s_{ki}[U^{\mathrm{II}}_{yz}]: \quad a^s_{10} = 5\nu-2, \quad a^s_{11} = 2-3\nu, \quad a^s_{20} = -8\nu, \quad a^s_{21} = -16(1-\nu), \quad a^s_{22} = 8(2-\nu) \tag{38}$$

$$a^s_{ki}[U^{\mathrm{III}}_{xy}]: \quad a^s_{10} = -2\nu+2, \quad a^s_{11} = -2, \quad a^s_{21} = 16, \quad a^s_{22} = -16 \tag{39}$$

$$a^c_{ki}[U^{\mathrm{III}}_{yz}]: \quad a^c_{00} = 2+\nu, \quad a^c_{10} = -32, \quad a^c_{11} = 32-4\nu, \quad a^c_{20} = 32, \quad a^c_{21} = -32. \tag{40}$$

The next step in the evaluation of integrals (31)–(33) is to expand r_u, r_l and b_k appearing in (34) in powers of $\sin\theta$ and $\cos\theta$. This allows us to express the integrals (31)–(33) as multiple sums involving powers of $\sin\theta$ and $\cos\theta$, but we find that the resulting expressions for $K^S_{\mathrm{I}}(0)$ are too cumbersome to be of any practical use thereby negating any advantage this procedure may have over the direct numerical integration of (15)–(17) that will be presented below. However, for a spheroidal region ($a = b$) centred at the origin, the integrals (31)–(33) can in fact be evaluated as a single infinite sum using the procedure involving expansion in powers of $\sin\theta$ and $\cos\theta$.

In this special case, it can be shown that the only non-zero components of the fundamental fields U^{I}_{mn} are U^{II}_{xy} and U^{III}_{yz}. Therefore, for constant transformation strains, we have

$$K^S_{\mathrm{I}} = 0 \tag{41}$$

$$K^S_{\mathrm{II}}(0) = \frac{2}{(1+\nu)}\varepsilon^T_{xy}\int_V U^{\mathrm{II}}_{xy}\,\mathrm{d}V \tag{42}$$

$$K^S_{\mathrm{III}}(0) = \frac{2}{(1+\nu)}\varepsilon^T_{yz}\int_V U^{\mathrm{III}}_{yz}\,\mathrm{d}V \tag{43}$$

where V: $x^2 + y^2 + \frac{a^2}{c^2}z^2 \leqslant 1$.

Oblate spheroid, $a > c$

$$K^S_{\mathrm{I}}(0) = 0 \tag{44}$$

$$\begin{aligned} K^S_{\mathrm{II}}(0) = -\frac{8\sqrt{2}}{(2-\nu)(1+\nu)}C_0\frac{c}{a}\varepsilon^T_{xy}\sum_{m=0}^{\infty}\left(1-\frac{c^2}{a^2}\right)^m\left\{\frac{4}{5}(2-3\nu)B\left(\frac{3}{4}, m+\frac{1}{2}\right)\right. \\ \left. + \frac{16}{15}(1+\nu)(m+1)B\left(\frac{7}{4}, m+\frac{1}{2}\right) - \frac{64}{105}(11-9\nu)\binom{m}{-3}B\left(\frac{11}{4}, m+\frac{1}{2}\right)\right\} \end{aligned} \tag{45}$$

$$K_{III}^S(0) = \frac{4\sqrt{2}(1-\nu)}{(2-\nu)(1+\nu)} C_0 \frac{c}{a} \varepsilon_{yz}^T \sum_{m=0}^{\infty} \left(1-\frac{c^2}{a^2}\right)^m \left\{-(2+\nu)B\left(\frac{3}{4}, m+\frac{1}{2}\right) + \frac{4}{3}(16+\nu)(m+1)B\left(\frac{7}{4}, m+\frac{1}{2}\right) - \frac{64}{3}\binom{m}{-3} B\left(\frac{11}{4}+m, \frac{1}{2}\right)\right\}. \quad (46)$$

Prolate spheroid, $a < c$

$$K_I^S(0) = 0 \quad (47)$$

$$K_{II}^S(0) = -\frac{8\sqrt{2}}{(2-\nu)(1+\nu)} C_0 \frac{a}{c} \varepsilon_{xy}^T \sum_{m=0}^{\infty} \left(1-\frac{a^2}{c^2}\right)^m \left\{\frac{4}{5}(2-3\nu)B\left(\frac{3}{4}+m, \frac{1}{2}\right) + \frac{16}{15}(1+\nu)(m+1)\frac{a^2}{c^2} B\left(\frac{7}{4}+m, \frac{1}{2}\right) - \frac{64}{105}(11-9\nu)\binom{m}{-3} \frac{a^4}{c^4} B\left(\frac{11}{4}+m, \frac{1}{2}\right)\right\} \quad (48)$$

$$K_{III}^S(0) = \frac{4\sqrt{2}(1-\nu)}{(2-\nu)(1+\nu)} C_0 \frac{a}{c} \varepsilon_{yz}^T \sum_{m=0}^{\infty} \left(1-\frac{a^2}{c^2}\right)^m \left\{-(2+\nu)B\left(\frac{3}{4}+m, \frac{1}{2}\right) + \frac{4}{3}(16+\nu)(m+1)\frac{a^2}{c^2} B\left(\frac{7}{4}+m, \frac{1}{2}\right) - \frac{64}{3}\binom{m}{-3} \frac{a^4}{c^4} B\left(\frac{11}{4}+m, \frac{1}{2}\right)\right\}. \quad (49)$$

Sphere, $a = c$

$$K_I^S(0) = 0 \quad (50)$$

$$K_{II}^S(0) = \frac{2\sqrt{2}}{(2-\nu)(1+\nu)} C_0 \varepsilon_{xy}^T \left(\frac{32}{9} - \frac{16}{5}\nu\right) B\left(\frac{3}{4}, \frac{1}{2}\right) \quad (51)$$

$$K_{III}^S(0) = \frac{8\sqrt{2}(1-\nu)}{5(2-\nu)(1+\nu)} C_0 \varepsilon_{yz}^T \left(\frac{38}{9} - \nu\right) B\left(\frac{3}{4}, \frac{1}{2}\right). \quad (52)$$

In (44)–(52)

$$B(p, q) = \int_0^1 x^{p-1}(1-x)^{q-1}\, dx. \quad (53)$$

The analytical expressions (50)–(52) were also useful for checking the accuracy of the general numerical integration procedure which is described in the next section.

4. NUMERICAL RESULTS AND DISCUSSION

For an arbitrary ellipsoidal domain V centred at x_0, y_0, z_0

$$(x-x_0)^2 + \frac{a^2}{b^2}(y-y_0)^2 + \frac{a^2}{c^2}(z-z_0)^2 \leqslant 1 \quad (54)$$

and constant transformation strains ε_{mn}^T, the integrals (15)–(17) were evaluated numerically using the Gaussian method. To enhance the rate of convergence of the singular integrals as $R \to 0$, ellipsoidal coordinates (20) were chosen which allowed formal integration of (15)–(17) with respect to the coordinate r such that the integrands took the form

$$(\sqrt{r_u} - \sqrt{r_l}) f(\theta, \bar{\phi}) \tag{55}$$

where the upper and lower limits of integration on r are given by (23). The ranges of integration with respect to θ and $\bar{\phi}$ given by expressions (25)–(29) were each divided into $2^3 = 8$ intervals, with each interval being represented by six Gauss points.

The accuracy of the numerical integration scheme was checked in two ways. First, by comparing with the analytical results (50)–(52). It was found that the numerical results differed from these by less than ± 0.01. Secondly, by increasing the number of intervals to $2^4 = 16$. It was found that the results hardly differed from those obtained with only $2^3 = 8$ intervals.

The numerical integration scheme was used for an exploration of the problem at hand for a general ellipsoidal domain V. In particular, attention was focussed on the spherical domain ($a = b = c$) and the oblate spheroidal domain with $a = b$ and $a/c = 5$. The choice of these two shapes was dictated by the fact that zirconia particles are spherical when found in an alumina matrix or as thin oblate spheroids when found in partially stabilized zirconia.

In an extensive numerical exploration of complex and singular integrals it is essential to have at least some independent checks on the qualitative, if not the quantitative, accuracy of the results. This was done by a close examination of the properties of U^{α}_{mn} appearing in integrals (15)–(17). It was found, for instance, that U^{α}_{mn} possess several symmetry properties with respect to y and z which influence the final result (i.e. K^S_{α}). The behaviour of U^{α}_{mn} with respect to y and z for various m, n and α is evident from Table 2. Moreover, it was found that

$$\begin{aligned} K^S_{\mathrm{I}}(-y) &= -K^S_{\mathrm{I}}(y); \quad z_0 = 0 \\ K^S_{\mathrm{I}}(-z) &= -K^S_{\mathrm{I}}(z); \quad y_0 = 0 \\ K^S_{\mathrm{II}}(-y) &= K^S_{\mathrm{II}}(y); \quad z_0 = 0. \end{aligned} \tag{56}$$

Finally, it was found that the dominant contributions to K^S_{I}, K^S_{II} and K^S_{III} came from U^{I}_{xy}, U^{II}_{xz} and U^{III}_{xz}, respectively. The remaining U^{α}_{mn} made but little contribution to K^S_{α}. Therefore, K^S_{I}, K^S_{II}, K^S_{III} exhibited essentially the respective symmetry behaviour of U^{I}_{xy}, U^{II}_{xz} and U^{III}_{xz} (Table 2). This observation was useful not only for performing a qualitative check on the numerical results, but also in simplifying the graphical presentation of the latter, in that the stress intensity factors could be plotted to within a factor of the strain ε^T_{mn} corresponding to the dominant U^{α}_{mn}. Thus in the figures to follow, the scale for K^S_{I} should actually be read as $K^S_{\mathrm{I}}/\varepsilon^T_{xy}$. In dimensioned quantities this scale represents $(K^S_{\mathrm{I}} E\sqrt{a})/\varepsilon^T_{xy}$. Similarly, the scale for K^S_{II} in dimensioned quantities should read $(K^S_{\mathrm{II}} E\sqrt{a})/\varepsilon^T_{xz}$, and for K^S_{III} should read $(K^S_{\mathrm{III}} E\sqrt{a})/\varepsilon^T_{xz}$.

It is now possible to comment on the typical behaviour of K^S_{α} as demonstrated by the numerical integration procedure ($\nu = 0.3$). This behaviour was found to be qualitatively totally consistent with the above observations. Typically, $|K^S_{\mathrm{I}}|$ for $a/c = 1$ was found to be consistently larger than that for $a/c = 5$ (Fig. 3). However, the variation of $|K^S_{\mathrm{I}}|$ with $|z_0| > 0$ was similar for both shapes; $|K^S_{\mathrm{I}}|$ decreased with increasing $|z_0| \geqslant 0$, initially rather slowly but then more rapidly.

Table 2. Behaviour of U^{α}_{mn}

mn	$\alpha = \mathrm{I}$	$\alpha = \mathrm{II}$	$\alpha = \mathrm{III}$
xy	$U^{\mathrm{I}}_{xy}(-y) = -U^{\mathrm{I}}_{xy}(y)$ $U^{\mathrm{I}}_{xy}(-z) = U^{\mathrm{I}}_{xy}(z)$	$U^{\mathrm{II}}_{xy}(-y) = U^{\mathrm{II}}_{xy}(y)$ $U^{\mathrm{II}}_{xy}(-z) = U^{\mathrm{II}}_{xy}(z)$	$U^{\mathrm{III}}_{xy}(-y) = U^{\mathrm{III}}_{xy}(y)$ $U^{\mathrm{III}}_{xy}(-z) = -U^{\mathrm{III}}_{xy}(z)$
yz	$U^{\mathrm{I}}_{yz}(-y) = -U^{\mathrm{I}}_{yz}(y)$ $U^{\mathrm{I}}_{yz}(-z) = -U^{\mathrm{I}}_{yz}(z)$	$U^{\mathrm{II}}_{yz}(-y) = U^{\mathrm{II}}_{yz}(y)$ $U^{\mathrm{II}}_{yz}(-z) = -U^{\mathrm{II}}_{yz}(z)$	$U^{\mathrm{III}}_{yz}(-y) = U^{\mathrm{III}}_{yz}(y)$ $U^{\mathrm{III}}_{yz}(-z) = U^{\mathrm{III}}_{yz}(z)$
zx	$U^{\mathrm{I}}_{zx}(-y) = -U^{\mathrm{I}}_{zx}(y)$ $U^{\mathrm{I}}_{zx}(-z) = -U^{\mathrm{I}}_{zx}(z)$	$U^{\mathrm{II}}_{zx}(-y) = -U^{\mathrm{II}}_{zx}(y)$ $U^{\mathrm{II}}_{zx}(-z) = -U^{\mathrm{II}}_{zx}(z)$	$U^{\mathrm{III}}_{zx}(-y) = -U^{\mathrm{III}}_{zx}(y)$ $U^{\mathrm{III}}_{zx}(-z) = U^{\mathrm{III}}_{zx}(z)$

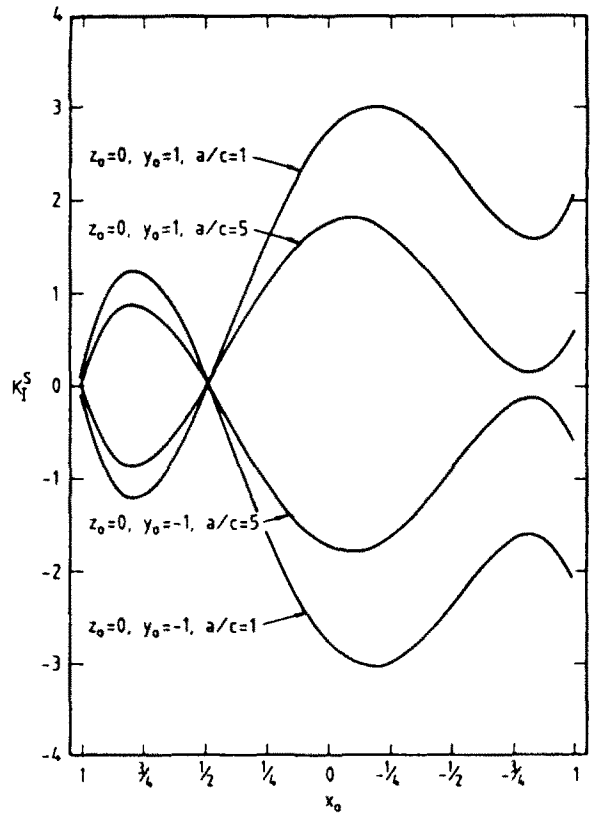

Fig. 3. Variation of $K_I^S(0)$ with x_0 for two typical values of y_0 and of a/c ($a = b$).

The shape of region V has a far more pronounced influence upon $|K_{II}^S|$ than upon $|K_I^S|$. $|K_{II}^S|$ for $a/c = 5$ is not only much smaller than for $a/c = 1$ but it diminishes rapidly with increasing $|z_0| > 0$. For $a/c = 1$, $|K_{II}^S|$ seems to achieve (Fig. 4) the maximum value at or near $|z_0| = 1/2$ and then decreases with increasing $|z_0| > 1/2$.

As far as $|K_{III}^S|$ is concerned, the shape and location of V seems to have an effect on it similar to that on $|K_I^S|$. Thus, $|K_{III}^S|$ for $a/c = 1$ is consistently larger than for $a/c = 5$ (Fig. 5). However, for both shapes it decreases with increasing $|z_0| > 0$, although the rate of decrease is different. For $a/c = 5$, it decreases rapidly with increasing $|z_0| > 0$, but for $a/c = 1$ it decreases rather slowly in the beginning.

Up to now, we were only interested in the shape of the transformation domain. We found in particular that spherical particles give a larger $|K_x^S|$ than do oblate spheroids with long axis normal to the crack front (i.e. parallel to x-direction).

It is known however (Lambropoulos, 1986), that the orientation of the long axis of oblate spheroids relative to the crack plane has a significant influence on the extent of change in K_x due to dilatational transformation strains. It is therefore of some interest to examine the influence of orientation of oblate spheroids on the stress intensity factors K_x^S due to shear transformations strain. We consider an additional orientation, namely when the long axis is parallel to the crack front (i.e. parallel to z-direction). An example of this orientation of oblate spheroids which corresponds in size to the previously considered orientation (long axis parallel to x-direction) is simulated by choosing $a = b$, $a/c = 0.2$.

When the long axis is parallel to the crack front (i.e. parallel to z-direction) numerical computations for $a = b$, $a/c = 0.2$ show, as expected, that the variation of $K_x^S(0)$ is more pronounced with $|z_0|$ than was the case for $a = b$, $a/c = 5$. Thus the maximum value of $|K_I|$ increases from around 4 at $z_0 = 0$ to about 14 at $|z_0| = 0.5$ and further to about 75 at $|z_0| = 1.0$. The increase is even greater in $|K_{II}|$. Its maximum value increases from about 0.6 at $z_0 = 0$ through about 22 at $|z_0| = 0.5$ to about 850 at $|z_0| = 1.0$. The largest increase is noticed in $|K_{III}|$. Its maximum value increases from about 8 at $z_0 = 0$ through about 14

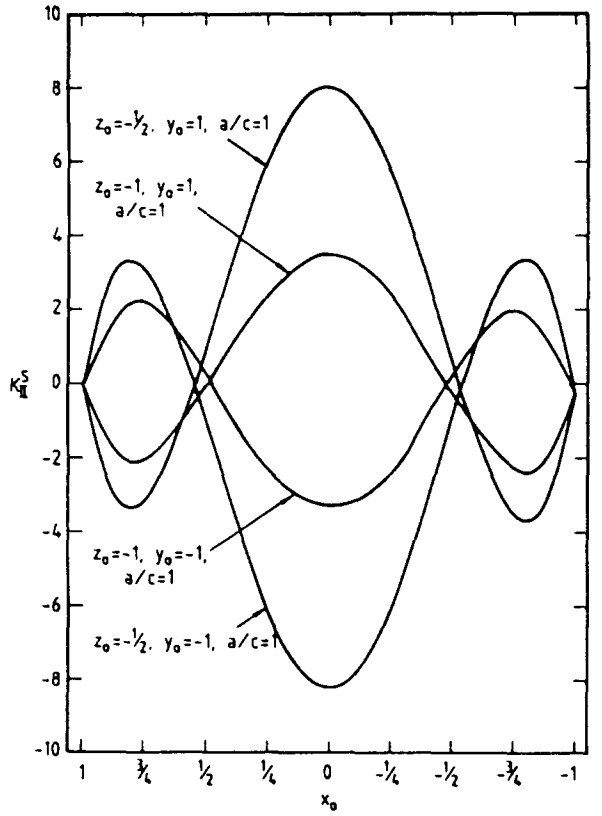

Fig. 4. Variation of $K_{II}^S(0)$ with x_0 for two typical values of y_0 and z_0 for a spherical region ($a = b = c$).

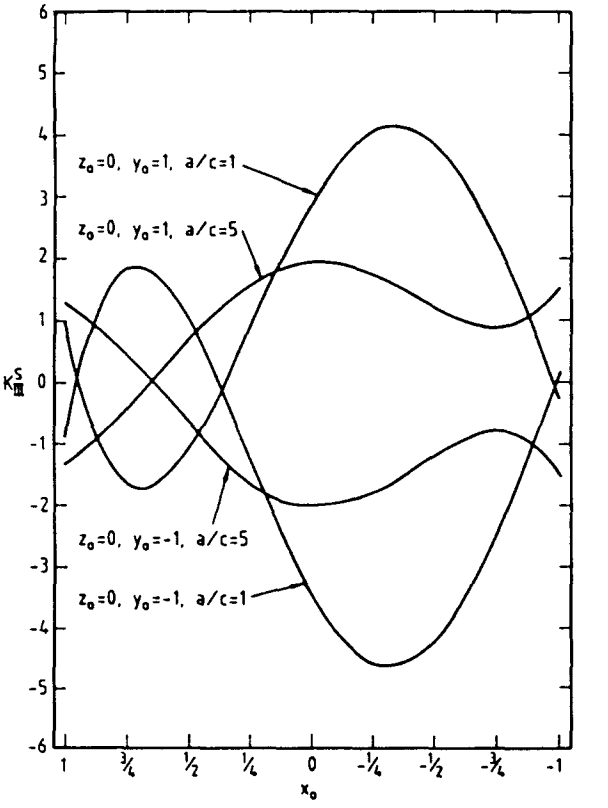

Fig. 5. Variation of $K_{III}^S(0)$ with x_0 for two typical values of y_0 and of a/c ($a = b$).

at $|z_0| = 0.5$ to a colossal 1850 at $|z_0| = 1.0$. This behaviour is quite consistent with that expected from analytical considerations.

Similar changes to $K_x^S(0)$ can be expected when the long axis is normal to the crack plane (i.e. parallel to y-direction). In conclusion, it should be added that further in-depth numerical exploration is in progress to gain a deeper insight into the extent of variation in $K_x^S(z')$ due to changes in the position and orientation of V. In particular, attempts are being made to derive useful analytical expressions for $K_x^S(z')$ in the limit as $\Delta V \to 0$.

Acknowledgement—We are grateful to Professor J. R. Rice for giving us draft and final copies of the report by Gao (1988).

REFERENCES

Budiansky, B. (1983). Micromechanics I. *Comput. Struct.* **16**, 3–12.
Budiansky, B., Hutchinson, J. W. and Lambropoulos, J. C. (1983). Continuum theory of dilatant transformation toughening in ceramics. *Int. J. Solids Structures* **19**, 337–355.
Bueckner, H. F. (1987). Weight functions and fundamental fields for the penny-shaped and half-plane crack in three-space. *Int. J. Solids Structures* **23**, 57–93.
Gao, H. (1988). Application of 3-dimensional weight functions—I. Report, Division of Applied Sciences, Harvard University, May 1987 (revised February 1988).
Lambropoulos, J. C. (1986). Shear, shape and orientation effects in transformation toughening. *Int. J. Solids Structures* **22**, 1083–1106.
McMeeking, R. M. and Evans, A. G. (1982). Mechanics of transformation toughening in brittle materials. *J. Am. Ceramics Soc.* **65**, 242–246.
Rice, J. R. (1985). Three dimensional elastic crack tip interactions with transformation strains and dislocations. *Int. J. Solids Structures* **21**, 781–791.

APPENDIX A

For an arbitrary domain V, U_{xz}^{I} and therefore K_I^S will contain the term $\mathrm{Re}\, G_{xzz}$ which may be rewritten in a non-dimensional form

$$\begin{aligned}\mathrm{Re}\, G_{xzz} &= \mathrm{Re}\, Q_{xz} + \mathrm{Im}\, G_{xzz} \\ &= 2C_0 \frac{q(z-z')}{R^4} + \mathrm{Im}\, G_{xzz}.\end{aligned} \tag{A1}$$

Likewise, U_{xz}^{II} and U_{xz}^{III}, and therefore K_{II}^S and K_{III}^S will contain the terms $\mathrm{Re}\, G_{xxz}$ and $\mathrm{Im}\, G_{xxz}$, respectively, which may be rewritten as

$$\begin{aligned}\mathrm{Re}\, G_{xxz} &= -\mathrm{Re}\, P_{xz} - \mathrm{Re}\, G_{xzz} \\ &= -C_0 \frac{q(z-z')}{R^4}\left\{1 - 8\frac{\rho^2}{R^2}(1-\cos\phi)\right\} - \mathrm{Re}\, G_{xzz}\end{aligned} \tag{A2}$$

$$\begin{aligned}\mathrm{Im}\, G_{xxz} &= -\mathrm{Im}\, P_{xz} - \mathrm{Im}\, G_{xzz} \\ &= -C_0 \frac{q}{2\rho^2 R^2}\left\{(-1+2\cos\phi) - (10-8\cos\phi)\frac{\rho^2}{R^2} + 16(1-\cos\phi)\frac{\rho^4}{R^4}\right\} - \mathrm{Im}\, G_{xzz}.\end{aligned} \tag{A3}$$

In (A1)–(A3), $Q = G_{xx} + iG_{xy}$ and $P = G_{xy}$.

To complete the discussion, it only remains to express explicitly G_{xzz} and G_{xzz}. We begin with G_{xzz}.

$$\begin{aligned}G_{xzz} &= G_{xzz}\zeta_z^2 + G_{xz}\zeta_{zz} \\ &= -\frac{C_0 q}{d^2 R^2}\left\{(2\rho - x) + 2\frac{\rho^2}{R^2}(x-\rho) - \frac{3}{2}\left[(2x-\rho) + 2\frac{x^2}{d^2}(-x+\rho)\right]\right\} \\ &\quad - i\frac{C_0 q(z-z')}{d^2 R^2}\left\{1 - 2\frac{\rho^2}{R^2}(1-\cos\phi) + \frac{3}{2}\left[1 - 2\frac{\rho^2}{d^2}\cos\phi(\cos\phi - 1)\right]\right\} - \frac{3}{4}\frac{G}{\zeta^4}\end{aligned} \tag{A4}$$

where

$$d = \sqrt{[x^2 + (z-z')^2]}$$

and

$$\operatorname{Re}\frac{G}{\zeta^4} = C_0\left\{\operatorname{Re}\omega\ \operatorname{Re}\frac{1}{\zeta^5} - \operatorname{Im}\omega\ \operatorname{Im}\frac{1}{\zeta^5}\right\}$$

$$\operatorname{Im}\frac{G}{\zeta^4} = C_0\left\{\operatorname{Re}\omega\ \operatorname{Im}\frac{1}{\zeta^5} + \operatorname{Im}\omega\ \operatorname{Re}\frac{1}{\zeta^5}\right\}. \tag{A5}$$

In (A5)

$$\omega = \ln\frac{q+\zeta}{q-\zeta}$$

such that

$$G(x, y, z-z') = \frac{C_0}{\zeta}\omega$$

and

$$\operatorname{Re}\omega = \frac{1}{2}\ln\frac{q^2+d+q\sqrt{[2(d+x)]}}{q^2+d-q\sqrt{[2(d+x)]}}$$

$$\operatorname{Im}\omega = \sin^{-1}\frac{2q\ \operatorname{Im}\zeta}{\sqrt{[(q^2-d)^2+(2q\ \operatorname{Im}\zeta)^2]}} \tag{A6}$$

$$\operatorname{Re}\frac{1}{\zeta^5} = \frac{1}{d^4d^{1/2}}\left\{\left(\frac{d+x}{2d}\right)^{1/2}[x^2-(z-z')^2] \pm 2\left(\frac{d-x}{2d}\right)^{1/2}x(z-z')\right\}$$

$$\operatorname{Im}\frac{1}{\zeta^5} = \frac{1}{d^4d^{1/2}}\left\{-2\left(\frac{d+x}{2d}\right)^{1/2}x(z-z') \pm \left(\frac{d-x}{2d}\right)^{1/2}[x^2-(z-z')^2]\right\} \tag{A7}$$

where the "$-$" sign is chosen when $(z-z') < 0$.

Finally, $G_{,zzz}$ is given by

$$\begin{aligned}
G_{,zzz} = {} & \frac{2C_0qz}{d^2R^4}\left\{\left(2\rho+\frac{3}{2}\rho-4x\right)+\left(\frac{1}{d^2}+\frac{2}{R^2}\right)(2\rho^2)(x-\rho)\right\} \\
& + \frac{2C_0qz}{d^4R^2}\left\{\left(2\rho+\frac{3}{2}\rho-4x\right)+\left(\frac{1}{R^2}+\frac{2}{d^2}\right)(-3x^2)(\rho-x)\right\} \\
& - i\frac{C_0q}{d^2R^2}\left\{1+\frac{3}{2}-2\frac{\rho^2}{R^2}(1-\cos\phi)-3\frac{\rho^2}{d^2}\cos\phi\ (\cos\phi-1)\right\} \\
& + i\frac{2C_0qz^2}{d^2R^4}\left\{1+\frac{3}{2}-2\rho^2(1-\cos\phi)\left(\frac{1}{d^2}+\frac{2}{R^2}\right)\right\} \\
& + i\frac{2C_0qz^2}{d^4R^2}\left\{1+\frac{3}{2}-3\rho^2\cos\phi\ (\cos\phi-1)\left(\frac{1}{R^2}+\frac{2}{d^2}\right)\right\} \\
& - i\frac{3C_0q}{4d^4R^2}\left\{4\frac{x^2}{d^2}[\rho x+(z-z')^2]-[3\rho x+(z-z')^2]\right\} \\
& + \frac{3}{4}\frac{C_0q(z-z')}{d^4R^2}\left\{(\rho-3x)+4\frac{x^2}{d^2}(x-\rho)\right\}+i\frac{15}{8}\frac{G}{\zeta^6}
\end{aligned} \tag{A8}$$

where

$$\operatorname{Re}\frac{G}{\zeta^6} = C_0\left\{\operatorname{Re}\omega\ \operatorname{Re}\frac{1}{\zeta^7} - \operatorname{Im}\omega\ \operatorname{Im}\frac{1}{\zeta^7}\right\}$$

$$\operatorname{Im}\frac{G}{\zeta^6} = C_0\left\{\operatorname{Re}\omega\ \operatorname{Im}\frac{1}{\zeta^7} + \operatorname{Im}\omega\ \operatorname{Re}\frac{1}{\zeta^7}\right\} \tag{A9}$$

and

$$\operatorname{Re}\frac{1}{\zeta^7} = \frac{1}{d^6d^{1/2}}\left\{\left(\frac{d+x}{2d}\right)^{1/2}[x^3-3x(z-z')^2] \pm \left(\frac{d-x}{2d}\right)^{1/2}(z-z')[3x^2-(z-z')^2]\right\}$$

$$\operatorname{Im}\frac{1}{\zeta^7} = \frac{1}{d^6d^{1/2}}\left\{-\left(\frac{d+x}{2d}\right)^{1/2}(z-z')[3x^2-(z-z')^2] \pm \left(\frac{d-x}{2d}\right)^{1/2}[x^3-3x(z-z')^2]\right\}. \tag{A10}$$

APPENDIX B

In order to prove that the last term in each of the three expressions (15)–(17) vanishes when ε_{zz}^r is a function of y alone, consider the region V with the closed, smooth surface

$$\begin{aligned} y_1 &\leqslant y \leqslant y_2 \\ x_1(y) &\leqslant x \leqslant x_2(y) \\ z_1(x,y) &\leqslant z \leqslant z_2(x,y). \end{aligned} \tag{B1}$$

Within the region V consider the subregion V' consisting of the torus ω (surface $x^2+y^2=\varepsilon^2$, $\varepsilon \ll 1$), and certain portions of the crack faces C^+, C^- and the region V. Bueckner (1987) has shown that $G(x,y,z)$ and $G_{,x}$ are harmonic in V', and $G(x,0,z)$ and $G_{,x}(x,0,z)$ are harmonic on C^+, C^- and ω. He has further shown that

$$\lim_{\varepsilon \to 0} \int_{V'} \ldots \mathrm{d}V = \int_V \ldots \mathrm{d}V. \tag{B2}$$

Referring to Fig. 2 and assuming in the first instance $z_1(0,0) \neq 0$ and $z_2(0,0) \neq 0$, we have

$$\begin{aligned} &\int_V \varepsilon_{zz}^r(y) G_{,zz}(x,y,z)\,\mathrm{d}x\,\mathrm{d}y\,\mathrm{d}z \\ &= \int_S \mathrm{d}x\,\mathrm{d}y\,\varepsilon_{zz}^r(y)[G_{,z}(x,y,z_2(x,y)) - G_{,z}(x,y,z_1(x,y))] \\ &= \int_{y_1}^{y_2} \varepsilon_{zz}^r(y)[G(x_2(y),y,z_2(x_2(y),y)) - G(x_1(y),y,z_2(x_1(y),y)) \\ &\quad - G(x_2(y),y,z_1(x_2(y),y)) + G(x_1(y),y,z_1(x_1(y),y))]\,\mathrm{d}y \\ &\quad - \int_{-\varepsilon}^{\varepsilon} \varepsilon_{zz}^r(y)[G(\sqrt{(\varepsilon^2-y^2)},y,z_2(\sqrt{(\varepsilon^2-y^2)},y)) - G(-\sqrt{(\varepsilon^2-y^2)},y,z_2(-\sqrt{(\varepsilon^2-y^2)},y)) \\ &\quad - G(\sqrt{(\varepsilon^2-y^2)},y,z_1(\sqrt{(\varepsilon^2-y^2)},y)) + G(-\sqrt{(\varepsilon^2-y^2)},y,z_1(-\sqrt{(\varepsilon^2-y^2)},y))]\,\mathrm{d}y. \end{aligned} \tag{B3}$$

The first integral in the right-hand side of (B3) vanishes because of continuity conditions

$$\begin{aligned} z_1(x_1(y),y) &= z_2(x_1(y),y) \\ z_1(x_2(y),y) &= z_2(x_2(y),y), \end{aligned} \tag{B4}$$

and so gives (with $|\theta| < 1$)

$$\begin{aligned} \int_{V'} \varepsilon_{zz}^r(y) G_{,zz}(x,y,z)\,\mathrm{d}V = &-2\varepsilon_{zz}^r(\theta\varepsilon)[G(\varepsilon\sqrt{(1-\theta^2)},\theta\varepsilon,z_2(\varepsilon\sqrt{(1-\theta^2)},\theta\varepsilon)) \\ &- G(-\varepsilon\sqrt{(1-\theta^2)},\theta\varepsilon,z_2(-\varepsilon\sqrt{(1-\theta^2)},\theta\varepsilon)) \\ &- G(\varepsilon\sqrt{(1-\theta^2)},\theta\varepsilon,z_1(\varepsilon\sqrt{(1-\theta^2)},\theta\varepsilon)) \\ &+ G(-\varepsilon\sqrt{(1-\theta^2)},\theta\varepsilon,z_1(-\varepsilon\sqrt{(1-\theta^2)},\theta\varepsilon))]\varepsilon. \end{aligned} \tag{B5}$$

Since $z_2(0,0) \neq 0$, $z_1(0,0) \neq 0$, it is clear from (B5) that

$$\lim_{\varepsilon \to 0} \int_{V'} \varepsilon_{zz}^r(y) G_{,zz}(x,y,z)\,\mathrm{d}V = 0. \tag{B6}$$

In a similar manner, it may be shown that

$$\lim_{\varepsilon \to 0} \int_{V'} \varepsilon_{zz}^r(y) y G_{,yyz}\,\mathrm{d}V = 0. \tag{B7}$$

We will now prove the results (B6), (B7) when $z_2(0,0) = 0$. In this case of course $z_1(0,0) \neq 0$.

From (B5) it is clear that $x \sim 0(\varepsilon)$ and $y \sim 0(\varepsilon)$. In view of the fact that S' is a quadratic surface it follows that $z \sim 0(\varepsilon)$. Consequently,

$$\zeta \sim 0(\sqrt{\varepsilon}), \quad q \sim 0(\sqrt{\varepsilon}), \quad \ln\frac{q+\zeta}{q-\zeta} \sim 0(1) \tag{B8}$$

and

$$G \sim \frac{1}{0(\sqrt{\varepsilon})}. \tag{B9}$$

In the right-hand side of (B5), the terms

$$G(\pm\varepsilon\sqrt{(1-\theta^2)}, \theta\varepsilon, z_2(\pm\varepsilon\sqrt{(1-\theta^2)}, \theta\varepsilon))\varepsilon \tag{B10}$$

can be shown to be of $0(\sqrt{\varepsilon})$. Therefore, these terms vanish as $\varepsilon \to 0$, and we recover the result (B6).

Likewise, in deriving the result (B7) we would encounter the terms

$$yG_{,x}(\pm\varepsilon\sqrt{(1-\theta^2)}, \theta\varepsilon, z_2(\pm\varepsilon\sqrt{(1-\theta^2)}, \theta\varepsilon))\varepsilon, \tag{B11}$$

which may be rewritten as

$$\varepsilon\eta\left[\frac{C_0 q}{\zeta^2(q^2-\zeta^2)} - \frac{C_0 q}{\rho(q^2-\zeta^2)} - \frac{G}{2\zeta^2}\right]. \tag{B12}$$

In view of (B8) and (B9), the term (B12) is of $0(\sqrt{\varepsilon})$. Therefore it will vanish as $\varepsilon \to 0$, and we recover the result (B7).